

Quantification of the vertical moisture transport in the sub cloud during transitions of Stratocumulus into Cumulus using LES-results

Coen Hennipman

Supervisors:
Dr. S.R. de Roode
Ir. J. J. van der Dussen

Clouds, Climate and Air Quality
Department of Multi-Scale Physics
Faculty of Applied Sciences
and
Department of Geoscience & Remote Sensing
Faculty of Civil Engineering and Geosciences

Abstract

In this thesis the moisture transport in a decoupled cloud has been investigated. Decoupling in this case means that the cloud topped boundary layer is not well mixed, and thereby some of the evaporated water at the sea surface will not reach the cloud. This research has been done by comparing different Large Eddy Solving models in the ASTEX-case and using DALES for 3 composite cases. LES-models solve the relevant equations on a certain grid-size and add explicitly an effect for the sub-grid level. To get an easy interpretable variable of the moisture flux profile, the moisture flux ratio is introduced. This ratio is defined as the moisture flux at a certain height divided by the moisture flux at the sea surface. The mean moisture ratio over time is an important parameter to use for the lifetime of the cloud. If not all the water that evaporates at the sea surface reaches the cloud, the lifetime and thereby the cloud cover is reduced. The resulting ratios are in the ASTEX-case: 0.89 at minimum cloud base and 0.99 at mean cloud base. In the composite cases is the minimum cloud base 0.85 and the mean cloud base 0.78. The minimum ratio never drops below 0.07, so there is always some upward turbulent moisture flux in the sub-cloud layer. Most important conclusion is the observable diurnal cycle. This indicates a high dependence on the radiation of the sun. During day a build-up of moisture in the surface mixed layer (SML) is observed, during night this moisture is transported till the cloud.

Contents

1	INTRODUCTION	6
2	THEORY.....	8
2.1	RELEVANT VARIABLES	8
2.1.1	<i>Specific Humidity.....</i>	8
2.1.2	<i>Potential Temperature</i>	8
2.1.3	<i>Virtual (Potential) Temperature.....</i>	9
2.1.4	<i>Liquid Water Potential Temperature.....</i>	10
2.1.5	<i>Summary of used Variables</i>	10
2.2	GOVERNING EQUATIONS	10
2.2.1	<i>Conservation of Mass.....</i>	10
2.2.2	<i>Conservation of Momentum.....</i>	10
2.2.3	<i>Conservation of Moisture and Heat.....</i>	11
2.3	TURBULENT FLUXES.....	11
2.3.1	<i>Tendency equation for the Moisture Flux.....</i>	11
2.3.2	<i>Liquid Water Potential Temperature Flux - Heat Flux.....</i>	12
2.3.3	<i>Virtual Potential Temperature Flux - Buoyancy Flux.....</i>	12
2.3.4	<i>Turbulent Kinetic Energy</i>	12
2.4	DECOUPLING	13
2.5	RELEVANT OBSERVABLES	14
2.5.1	<i>Cloud Fraction.....</i>	14
2.5.2	<i>Liquid Water Path</i>	14
2.5.3	<i>Buoyancy-flux Integral Ratio</i>	14
2.5.4	<i>Moisture Flux Ratio</i>	15
2.5.5	<i>Buoyancy Flux Ratio.....</i>	15
2.6	LARGE EDDY SIMULATING	15
3	MODEL RESULTS OF CLOUD TRANSITIONS	17
3.1	TRANSITION.....	17
3.1.1	<i>Cloud Fraction.....</i>	17
3.2	DECOUPLING	19
3.2.1	<i>Result of Profiles</i>	19
3.2.2	<i>Buoyancy Integral Ratio</i>	20
3.2.3	<i>Buoyancy Flux Ratio</i>	21
4	TURBULENT MOISTURE FLUX RATIO	22
4.1	HEIGHT DEPENDENCE OF THE TURBULENT MOISTURE FLUX RATIO	22
4.2	ASTEX RESULTS	22
4.3	COMPOSITE CASES RESULTS.....	24
5	CONCLUSIONS AND RECOMMENDATIONS.....	26
5.1	CONCLUSIONS.....	26
5.2	RECOMMENDATIONS	26
6	BIBLIOGRAPHY.....	28
7	APPENDIX A.....	30
	REYNOLDS DECOMPOSITION AND AVERAGING	30

1 Introduction

In recent times much research has been done to examine the transition from stratocumulus to cumulus in the subtropical parts of the ocean. During this transition the cloud cover will decrease. This is due to the different cloud cover for the different cloud types. Stratocumulus has a typical cloud cover of 100%, for cumulus this is 10%. A typical example of stratocumulus can be seen in Figure 1, for cumulus there is a typical example in Figure 2. An earlier transition would lead to in total lower cloud cover compared with a later transition. More cloud cover prevents radiation to reach and thereby heat the sea surface. Therefore the timespan of the transition will lead to changes in the total radiation that reach the earth, and thereby has consequences on the greenhouse effect. By better understanding the leading processes, a better sensitivity analyses can be done.



Figure 1 Stratocumulus



Figure 2 Cumulus

One of the important processes is the entrainment at the cloud top. Entrainment mixes dry and warm air from the thermal inversion layer above. This causes a gradual ascend of the cloud, partially compensated by subsidence, and the cloud will dry and thin. On the other hand, moisture evaporation from the sea surface could supply extra moisture which prolongs the lifetime of the stratocumulus cloud. Central objective of this research is to quantify the amount of moisture flux that reaches the stratocumulus cloud. Therefore the moisture flux ratio is introduced. This ratio, r_q , is the turbulent moisture transport at the cloud base divided by the moisture transport at the sea level.

The moisture flux ratio could be influenced by decoupling. Decoupling describes the case when the cloud-topped boundary layer (CTBL) can be separated in two layers. These separation exist when two layers do not mix and therefore evaporated water at the surface do not reach the upper part of the cloud. This separation can happen if there is a negative buoyancy at the cloud base. In this area the rising thermals from the sea surface will be damped. This negative buoyant area hinders the moisture flux from the sea surface to reach the cloud. The cloud will dry up earlier, because there is less moisture flux coming in from below. Various papers

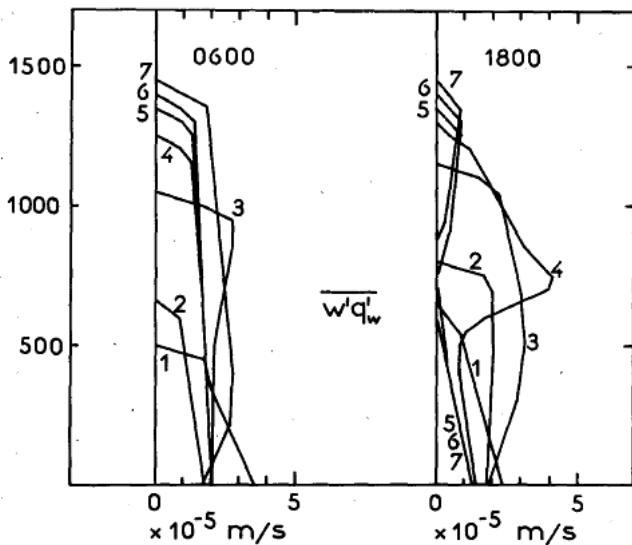


Figure 3 Bougeault 1985, figure 7. The turbulent flux of moisture at 0.600h and 18.00h, for subsequent days.

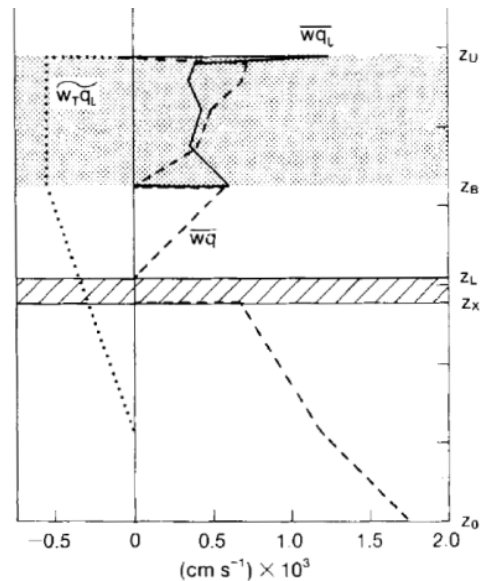


Figure 4 Turton and Nicholls 1987, figure 8d. Water substance flux at 10h, from the integration for mid-latitude stratocumulus in summer after seperation has occurred. (wq is the used notation for turbulent vapor flux)

(Bougeault, 1985, Turton and Nicholls, 1987, Martin et al., 1994) argue/assume that there is no moisture transport at the cloud base if there is decoupling. For convenience the summarizing plots Bougeault (1985) and Turton and Nicholls (1987) are added in Figure 3 and in Figure 4. The quote from Martin et al. (1994): 'The effect of decoupling on the stratocumulus cloud is to virtually cut off the cloud layer from the moisture source of the sea surface'.

Due to decoupling the profiles of the conserved variables are not flat anymore. Therefore the Mixed Layer Model (MLM), assuming the cloud well mixed, provides an inadequate description of the cloud. Therefore also the simulations based on MLM are not valid anymore. So instead of using the computational very easy MLM, a more advanced model has to be used. Turton and Nicholls (1987) use a 2 layer model instead. By using Large Eddy Solving (LES) models even the assumption of a 2 layer model is not needed. These LES-models solve the relevant physical equations on a certain grid-size and take explicitly the sub grid scale transport into account. The used 5 LES-models use different parameterizations. By using multiple models the differences among them can be acquired and also the common behavior. The differences can be used to construct a spread of the predictions. This spread can be used as a measure whether the simulations are correct, because it is more likely that if the models are close, the outcomes are correct.

The models are used to simulate 4 different cases. The first case is the Atlantic Stratocumulus Transition Experiment (ASTEX). This experiment was held in June 1992. During two days the transition of stratocumulus to cumulus was observed. At the start of the transition there is are stratocumulus clouds beginning at an height of around 500m. After a while the stratocumulus ascend and cumulus clouds below appear. At the end of the transition there are only cumulus clouds. The observational area is part of the so called Hadley circulation. This circulation can be found in Figure 5. The ASTEX-case is simulated by 5 different LES-models. An overview of these models is in Table 2.

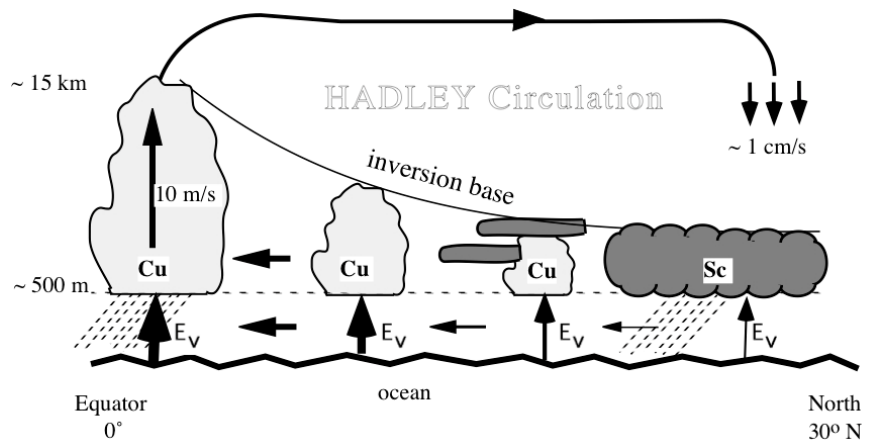


Figure 5 The Hadley Circulation

The other 3 cases are based on the trajectories of almost 10.000 air parcels in four subtropical oceans. These cases were combined into 3 composite cases. A selection was made based on the timescale of the transition. The three composite cases are: slow, ref(erence) and fast. The similarity with the ASTEX-case is the increase in the temperature of the sea surface and the transition from stratocumulus to cumulus. In the paper of Sandu (2010) a more detailed description of these composite cases is given. The composite cases have been simulated using the Dutch Atmospheric LES (DALES) model.

2 Theory

The description and modeling of clouds can be made much easier by introducing new variables and some mathematical tools. Why and how this variables are used can be found in 2.1. The used mathematical tools are Reynolds decomposition and Reynolds averaging. Both tools are widely used in cloud modeling. These tools are explained in Appendix A.

2.1 Relevant Variables

To make the modeling much easier and faster some new variables have to be introduced. These variables are conserved under different circumstances. To get the temperature independent of height and the corresponding pressure, the potential temperature is introduced. To get this variable conserved under different vapor amounts, the virtual potential temperature is added. The last added variable is the liquid water potential temperature, this variable is conserved during phase changes. Almost all these variables depend on the humidity, therefore first the specific humidity is introduced.

2.1.1 Specific Humidity

Water can appear in multiple phases. The sea consists of liquid water, directly above is water vapor present and in the clouds are both liquid water and water vapor. In our case we neglect the presence of ice, because the simulated cases are located near the equator and the considered clouds are not higher than 2,5 kilometer. The processes depend on the phase of the water, and therefore a distinction is made. This can be done by introducing the specific humidity. This variable is defined as

$$q_i = \frac{m_i}{m}. \quad (2.1)$$

Where i indicates water vapor, liquid water or total moisture, respectively by v , l or t . m_i is the mass of water in the specified phase and m is the total mass of the dry air and the water mass. The total mass is expressed in kilograms and the mass of water in the specified phase is expressed in grams. Some choose to express variable m_i in kilograms instead of grams, which introduces a factor 1000. Typical values for q_i are around 5-15 g/kg. If the air is saturated the following equation can be used

$$q_t = q_s + q_l. \quad (2.2)$$

In which q_s is the saturated humidity.

2.1.2 Potential Temperature

It is a common knowledge that the air pressure at higher altitudes is lower. This is due the gravitational force pulling molecules towards the earth. Through the gravitational force the pressure and the density of molecules are dependent on height. The vertical pressure gradient is described by

$$\frac{\partial p}{\partial z} = -\rho g. \quad (2.3)$$

Where p is the pressure, z the height, ρ the density and g of the gravitational acceleration. A rising air parcel will get a lower pressure. By using the ideal gas law it can be seen that a lower pressure leads to a lower temperature if there are no further changes. Using the same reasoning for a sinking air parcel leads to a higher temperature. The potential temperature is introduced to avoid temperature changes due to this effect.

To obtain the new variable the first law of thermodynamics has to be used, which is in incremental form

$$dh = T ds + \frac{dp}{\rho}. \quad (2.4)$$

Where h is the specific enthalpy, s the specific entropy and ρ the density. If we assume that the process is isentropic, and $dh = c_p dT$, where c_p is the specific heat at constant pressure, this equation simplifies to

$$c_p dT = \frac{dp}{\rho}. \quad (2.5)$$

By assuming that the ideal gas law is valid, and using the specific gas constant for dry air, R_d , the following equation is obtained

$$\frac{dp}{p} = \frac{c_p}{R} \frac{dT}{T}. \quad (2.6)$$

Integrating both sides leads to

$$\left(\frac{p_1}{p_0}\right)^{R/c_p} = \frac{T_1}{T_0}. \quad (2.7)$$

Solving for T_1 shows that if the air parcel is moved adiabatically to the pressure level p_1 , the potential temperature is given by

$$T_1 = T_0 \left(\frac{p_1}{p_0}\right)^{R/c_p} \equiv \theta. \quad (2.8)$$

This new variable has the disadvantage that it is obtained by using the assumption of dry air. Therefore this variable is only conserved if there is no phase transition. To remedy this, some new variables have to be introduced.

2.1.3 Virtual (Potential) Temperature

The previous derivation was based on the assumption of dry air. In most cases there will be water vapor and possibly some liquid water present. The presence of water influences the density. The density of water vapor is lower than the density of dry air. This can be seen by using the ideal gas law and knowing that H₂O has a lower molecular weight compared to the weighted mean of the other main components of dry air, namely: NO₂, O₂, Ar and CO₂. The density of liquid water is higher, which could result in an overall higher density. To get this in one variable, the virtual temperature is introduced. Parcels with a lower density are positively buoyant and are less attracted by gravitational force compared with negatively buoyant parcels. Therefore positively buoyant parcels are likely to rise and negatively buoyant parcels are likely to sink. The variable, T_v , is defined as the temperature a dry parcel of air would have if its pressure and temperature were equal to those of moist air. Which in equation form means

$$p = \rho R_d T_v = \rho R_m T. \quad (2.9)$$

Where R_d is the gas constant for dry air and R_m is the gas constant for the mixture. The gas constant of the mixture can be expressed as

$$R_m = (1 - q_v - q_l)R_d + q_v R_v. \quad (2.10)$$

To achieve this equation the volume of liquid water is neglected, because this volume is insignificant compared to the total volume. Substituting in eqn. (2.10) in (2.9) and rearranging terms gives the definition of T_v

$$T_v = T \left(1 - \left(1 - \frac{1}{\epsilon}\right)q_v - q_l\right). \quad (2.11)$$

In which $\epsilon = R_d/R_v \approx 0.622$. By simplifying the term in front of q_v and dividing both sides by the left hand side(lhs) of (2.7) provides the final definition for the virtual potential temperature,

$$\theta_v = \theta(1 + 0.61q_v - q_l). \quad (2.12)$$

A more extensive derivation of this variable can be found in appendix D of Stull (1993).

This variable can easily be used for the buoyancy of a parcel. This can be seen the following derivation starting with the ideal gas law,

$$T_v = \frac{p}{\rho R_d}. \quad (2.13)$$

Rewritten in its mean part and a deviation

$$(\overline{T_v} \overline{\rho} + \overline{T_v} \rho' + T_v' \overline{\rho} + T_v' \rho') R_d = \overline{p} + p'. \quad (2.14)$$

By neglecting the second order term on the lhs, and dividing everything by $\overline{\rho}$, the following equation is obtained

$$\left(\frac{\overline{T_v} \overline{\rho}}{\overline{\rho}} + \frac{\overline{T_v} \rho'}{\overline{\rho}} + \frac{T_v' \overline{\rho}}{\overline{\rho}}\right) R_d = 1 + \frac{p'}{\overline{p}}. \quad (2.15)$$

The last term on the right hand side (rhs) can be neglected. The first term on the lhs cancels due to the first term on the rhs. Leading to

$$\frac{T_v'}{\overline{T_v}} = -\frac{\rho'}{\overline{\rho}} = \frac{\theta_v'}{\overline{\theta_v}}. \quad (2.16)$$

Which perfectly shows that a variation of the virtual temperature is equivalent to a variation in density.

2.1.4 Liquid Water Potential Temperature

The potential temperature is not conserved when phase changes occur. In that case there has to be a correction term for the latent heat. The definition for the liquid water potential temperature, θ_l , is the temperature a parcel of air would get if all the water would be in the vapor phase thereby consuming the latent heat, and the parcel was brought adiabatically to a standard reference pressure. The liquid water potential temperature is given by

$$\theta_l \approx \theta - \frac{l_v}{c_p} q_l \quad (2.17)$$

Where l_v is the latent heat of vaporization of water. This variable, θ_l , is conserved in case of phase changes.

2.1.5 Summary of used Variables

The introduced variables are conserved under different conditions. The prior condition for conservation is that air parcels that are vertically displaced do not exchange heat with their environment. To get an overview of the introduced variables and their use see Table 1. Some others use also the 'virtual liquid potential temperature'. Because this variable is not used in the models, this variable will not be discussed here.

Table 1 Used Variables

Extended name	Used for	Symbol	Conserved for changes in
Potential Temperature	Temperature	θ	pressure
Virtual Potential Temperature	Buoyancy	θ_v	pressure
Liquid Water Potential Temperature	Heat	θ_l	pressure and phase
Total Moisture	Moisture	q_t	pressure and phase

2.2 Governing Equations

In the previous section some new variables are introduced. The main goal was to get variables conserved under different circumstances. Besides the conserved variables θ_l and q_t , the conserved variables mass and momentum are taken into account.

2.2.1 Conservation of Mass

Conservation of mass can be written as

$$\frac{\partial \rho}{\partial t} + \frac{\partial \rho u_j}{\partial x_j} = 0. \quad (2.18)$$

The index j indicates the sum over all directions or flows, x , y and z or u , v and w . This equation can be simplified by the assumption of incompressibility of air. The first term in (2.18) will be zero by that assumption. The result is then

$$\frac{\partial u}{\partial x} + \frac{\partial v}{\partial y} + \frac{\partial w}{\partial z} = 0. \quad (2.19)$$

2.2.2 Conservation of Momentum

Momentum is conserved in three directions. In the considered cases mainly the vertical component is of interest. The conservation of momentum equation in the vertical direction is

$$\frac{\partial w}{\partial t} + u_j \frac{\partial w}{\partial x_j} = -g - \frac{1}{\rho} \frac{\partial p}{\partial z} + \nu \frac{\partial^2 w}{\partial x_j^2}. \quad (2.20)$$

Where ν is the kinematic viscosity. The last term is a diffusion term. The total derivative is introduced to simplify this equation. The total derivative, sometimes called material derivative, is given by

$$\frac{d}{dt} = \frac{\partial}{\partial t} + u_j \frac{\partial}{\partial x_j}. \quad (2.21)$$

Using the total derivative for equation (2.20) gives

$$\frac{dw}{dt} = -g - \frac{1}{\rho} \frac{\partial p}{\partial z} + \nu \frac{\partial^2 w}{\partial x_j^2}. \quad (2.22)$$

Splitting this in a mean part and a fluctuating part and neglecting subsidence gives

$$\frac{dw'}{dt} = -\frac{\rho'}{\rho}g - \frac{1}{\rho}\frac{\partial p'}{\partial z} + \nu\frac{\partial^2 w'}{\partial x_j^2}. \quad (2.23)$$

Subsidence can be neglected because of the relatively small values of subsidence compared with the vertical velocity fluctuations. The first term on the rhs can be changed by using (2.16). This leads to a more used equation namely

$$\frac{dw'}{dt} = \frac{\theta_v'}{\theta_v}g - \frac{1}{\rho}\frac{\partial p'}{\partial z} + \nu\frac{\partial^2 u_j}{\partial x_j^2}. \quad (2.24)$$

The first term on the rhs relates the buoyancy and the flux. It can be seen that the sign of θ_v' is important. If θ_v' is positive this leads to a positive tendency for the flux, if it is negative it is a sink term. A more detailed description can be found in de Roode (2004).

2.2.3 Conservation of Moisture and Heat

The variables θ_j and q_t are conserved quantities. The general tendency equation of a conserved quantity is given by

$$\frac{\partial \varphi}{\partial t} + u_j \frac{\partial \varphi}{\partial x_j} = \nu_\varphi \frac{\partial^2 \varphi}{\partial x_j^2} + S_\varphi. \quad (2.25)$$

Where ν_φ is the molecular diffusivity of the conserved quantity φ , and S_φ is the net source/sink term due to processes for which the variable is not conserved. Equation (2.25) can be expanded into a mean and turbulent part, $\varphi = \bar{\varphi} + \varphi'$. After doing so applying Reynolds averaging gives

$$\frac{\partial \bar{\varphi}}{\partial t} + \bar{u}_j \frac{\partial \bar{\varphi}}{\partial x_j} = \nu_\varphi \frac{\partial^2 \bar{\varphi}}{\partial x_j^2} + S_\varphi - \frac{\partial \overline{u_j' \varphi'}}{\partial x_j}. \quad (2.26)$$

This equation is very similar to the previous one. The difference is that the variables are averaged and one term is added. This third term on the rhs represents the divergence due to turbulence. It is a correlation term between the fluctuation in velocity and the conserved variable. The variable φ could be substituted by q_t and θ_l , because both are conserved, leading to

$$\frac{\partial \bar{q}_t}{\partial t} + \bar{u}_j \frac{\partial \bar{q}_t}{\partial x_j} = \nu_{q_t} \frac{\partial^2 \bar{q}_t}{\partial x_j^2} + S_{q_t} - \frac{\partial \overline{u_j' q_t'}}{\partial x_j}, \quad (2.27)$$

and

$$\frac{\partial \bar{\theta}_l}{\partial t} + \bar{u}_j \frac{\partial \bar{\theta}_l}{\partial x_j} = \nu_{\theta_l} \frac{\partial^2 \bar{\theta}_l}{\partial x_j^2} + S_{\theta_l} - \frac{\partial \overline{u_j' \theta_l'}}{\partial x_j}. \quad (2.28)$$

2.3 Turbulent Fluxes

The relevant variables were defined and the governing conservations are derived. The presented derivation is more or less a summary/description of the derivation in Stull (1993). The entrainment, precipitation and radiation will not be discussed here. These processes are beyond the scope of this thesis, although they effect the simulations. A more extensive description of these processes in the ASTEX-case can be found in van der Dussen (2009).

2.3.1 Tendency equation for the Moisture Flux

The whole derivation of the moisture flux is too much to describe over here. Therefore the intermediate steps of the derivation are explained by words, instead of a derivation in formula form. To come to the moisture flux some previous equations have to be combined. The needed equations are the conservation of momentum (2.22) and the conservation of moisture (2.25). Both equations have to be split in mean and turbulent parts. Afterwards both equations have to be Reynolds averaged. These obtained equations have to be subtracted from the previously split equation. The resulting equation for the momentum has to be multiplied by the moisture perturbation and the resulting moisture equation has to be multiplied by the momentum perturbation. The resulting two equations have to be added. The pressure diffusion term and the molecular diffusion term are neglected because these are small compared to other terms. The resulting equation is

$$\frac{\partial}{\partial t} \overline{w' q_t'} + \bar{U}_j \frac{\partial}{\partial x_j} \overline{w' q_t'} = -\overline{u_j' q_t'} \frac{\partial \bar{w}}{\partial x_j} - \overline{w' u_j'} \frac{\partial \bar{q}_t}{\partial x_j} - \frac{\partial}{\partial x_j} \overline{w' u_j' q_t'} + g \frac{\overline{q' \theta_v'}}{\theta_v} + \frac{1}{\rho} \frac{\partial \overline{p' q_t'}}{\partial z} - 2\varepsilon_{wq}. \quad (2.29)$$

The index j indicates the sum over all directions or currents, x , y and z or u , v and w . This equation can be

simplified by the assumptions of horizontally homogeneity and no subsidence. The second assumption of no subsidence is in some cases not correct, but it is negligible in comparison with the moisture flux tendency. The budget equation of the moisture flux by using the assumption of horizontally homogeneity and no subsidence is

$$\frac{d}{dt} \overline{w'q_t'} = -\overline{w'^2} \frac{d\overline{q_t}}{dz} - \frac{d}{dz} \overline{w'w'q_t'} + \frac{g}{\theta_v} \overline{q_t'\theta_v'} + \left(\frac{1}{\rho}\right) \overline{p' \frac{dq_t'}{dz}} - 2\varepsilon_{wq_t}. \quad (2.30)$$

In this simplified equation the first term on the rhs provides a moisture flux in upward direction if the gradient is negative. A negative gradient means that the air above is dryer than below. This can be easily imagined, because if there is much turbulent flow, $\overline{w'^2}$ is high, and the gradient is negative, there will be an upward moisture flux. The $\overline{w'^2}$ term is by definition always positive. The second term is for the turbulent transport. The third term is a production term, the more correlation between wet and light parcels, the more moisture flux. The fourth term is a redistribution term and this provides a flow to relatively dry spaces. The last term is a dissipation term.

2.3.2 Liquid Water Potential Temperature Flux - Heat Flux

The derivation of the heat flux is similar to the moisture flux. The resulting expression, by using the same assumptions is

$$\frac{d}{dt} \overline{w'\theta_l'} = -\overline{w'^2} \frac{d\overline{\theta_l}}{dz} - \frac{d}{dz} \overline{w'w'\theta_l'} + \frac{g}{\theta_v} \overline{\theta_l'\theta_v'} + \left(\frac{1}{\rho}\right) \overline{p' \frac{d\theta_l'}{dz}} - 2\varepsilon_{w\theta_l}. \quad (2.31)$$

The terms have a similar interpretation as the moisture flux. A negative value for the heat flux can cause a negatively buoyant area as can be seen in the next paragraph.

2.3.3 Virtual Potential Temperature Flux - Buoyancy Flux

To obtain the buoyancy flux equation, the definition of virtual potential temperature (2.12) has to be split in its mean and turbulent part. Multiplying the obtained equation by w' , applying Reynolds averaging and neglecting third order terms results in

$$\overline{w'\theta_v'} = \overline{w'\theta'}(1 + 0.61\overline{q_v} - \overline{q_l}) + \overline{\theta'(0.61\overline{w'q_v'} - \overline{w'q_l'})}. \quad (2.32)$$

If there is no liquid water present, for example below the cloud, q_l is 0. The previous equation simplifies to

$$\overline{w'\theta_v'} = \overline{w'\theta'}(1 + 0.61\overline{q_v}) + 0.61\overline{\theta w'q_v'}. \quad (2.33)$$

The mean potential temperature can be estimated and in unsaturated conditions is the potential temperature equal to the liquid potential temperature. Using both leads to

$$\overline{w'\theta_v'} = A_d \overline{w'\theta_l'} + B_d \overline{w'q_t'} \quad (2.34)$$

Where $A_d \approx 1,01$ and $B_d \approx 180K$. Because there is no liquid water q_t and q_v can be exchanged.

If there is some liquid water present, the derivation is less straightforward. Therefore only the result of the derivation in Roode(2004) is shown. In a saturated atmosphere the virtual potential temperature flux is given by

$$\overline{w'\theta_v'} = A_w \overline{w'\theta_l'} + B_w \overline{w'q_t'}. \quad (2.35)$$

Where $A_w \approx 0.5$ and $B_w \approx 1100K$. A notable thing is the difference in coefficients for the saturated and unsaturated case. In saturated conditions the moisture flux is more important compared with the heat flux. In unsaturated conditions it is the other way around.

2.3.4 Turbulent Kinetic Energy

The turbulent kinetic energy (TKE) is defined as

$$\bar{e} = \frac{1}{2}(\overline{u'^2} + \overline{v'^2} + \overline{w'^2}). \quad (2.36)$$

In our case only the vertical component, w'^2 , is important. To derive a tendency equation for the TKE the same steps can be taken as for the moisture flux. The equation from the conservation of momentum (2.22) have to be split in mean and turbulent parts. After that apply Reynolds averaging and subtract this equation from the equation which is split in mean and turbulent part. Multiply this equation by w' and again apply Reynolds averaging. Smaller terms, such as diffusion, are neglected and after rewriting the following equation is obtained

$$\frac{d\overline{w^2}}{dt} = 2\frac{g}{\theta_v}\overline{w'\theta_v'} - \frac{\partial u_j'w'^2}{\partial x_j} - \frac{2}{\bar{\rho}}\frac{\partial}{\partial z}\overline{w'\rho'} - 2\varepsilon. \quad (2.37)$$

The first term on the rhs is the buoyancy production term, an important term for decoupling. Because when this term is smaller than zero, this is a sink term for the variance. The other terms are respectively: turbulent transport, pressure transport and dissipation. The pressure and turbulent transport terms redistribute, and the dissipation term is a sink term for the vertical turbulence.

2.4 Decoupling

The word ‘decoupling’, means there is separation between the sub-cloud layer below and the cloud layer above. Different degrees of separation are covered by the word decoupling. In this case the word ‘decoupling’ is used for the case that the layers do not mix. Normally clouds mix due to the presence of linear and turbulent flows. When there is decoupling, this is not the case.

In this paragraph the following equations are used:

- The buoyancy flux in eq. (2.34) and eq. (2.35).
- The moisture flux in eq. (2.30)
- The turbulent kinetic energy in eq. (2.37)

These equations are displayed below for convenience, without third order, redistribution and dissipation terms these equations simplify to

$$\overline{w'\theta_v'} = A\overline{w'\theta_l'} + B\overline{w'q_t'}; \quad \frac{d\overline{w^2}}{dt} = 2\frac{g}{\theta_v}\overline{w'\theta_v'}; \quad \frac{d}{dt}\overline{w'q_t'} = -\overline{w^2}\frac{dq_t}{dz} + \frac{g}{\theta_v}\overline{q_t'\theta_v'} \quad (2.38)$$

Typically there is a dry SML and above there is a region with some cumulus clouds. In the dry region the dry coefficients for the buoyancy flux have to be used and in the cloudy grid cells the wet coefficients. The buoyancy flux is an important factor in the decoupling process because it is a production term for w^2 . If the buoyancy flux is positive, positively buoyant air parcels rise. It is possible that the buoyancy flux becomes negative below the sub-cloud layer, most of the times due to a negative heat flux. This negative buoyant area leads to a decrease of w^2 . A decrease of the turbulence leads to a decrease in turbulent moisture transport, because the gradient of humidity with respect to height is typically negative. Thermals rising from the sea surface are hindered in the way up to the stratocumulus layer.

The decoupling can be observed in some different ways. Mostly the profiles of the different variables are shown to see the decoupling. Both the profiles of the fluxes and the of the conserved variables can be chosen

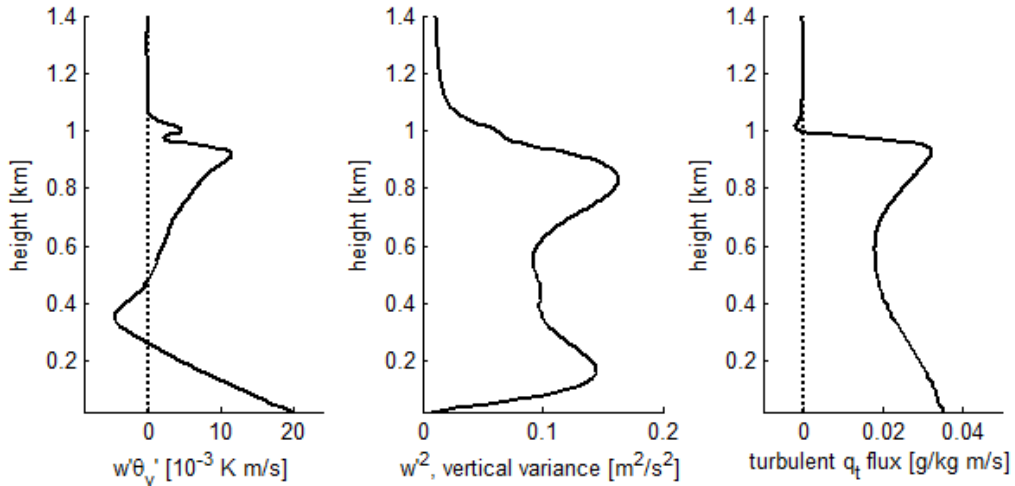


Figure 6 Typical example of Decoupling in DALES simulating ASTEX at 12h

do display the decoupling. A typical example is in Figure 6. The most used indication is the profile of the buoyancy flux. A negative buoyancy flux at the cloud base leads to a decrease in vertical turbulence. For a more quantitative description of this profile the Buoyancy Integral Ratio is used. The description of this ratio can be found in 2.5.3. A second indication of the decoupling is the profile of the moisture flux. From the sea surface there is typically an upward moisture flux. Above the cloud there is a layer without turbulence, so w' is 0, therefore there is no turbulent moisture flux. Below this layer there will be a linear flux if there is enough mixing. So if the flux is constant from the sea surface till the cloud top height the cloud is coupled. But if there is decoupling the moisture flux will be lower in the area below the cloud base. The last used flux profile is the variance. A same type of reasoning can be applied to this profile. In a mixed layer the vertical turbulence is high. A source for this vertical variance can be the entrainment from above and the evaporating water from below. Also radiation can cause vertical variance. In case of a mixed layer there will be one maximum of the variance located around half of the cloud. When there is some decoupling, the top will be less pronounced. If there is some more decoupling there arise a second top. For fully decoupled layers there is zero variance between these tops. Because of the definition of variance will zero variance not be reached, however it can reach approximately zero. Conserved variables will have the same value for different height through the whole mixed layer, differences in θ_l and q_t will be mixed away. If there is decoupling the profile of the conserved variable is no longer flat.

2.5 Relevant Observables

To describe the cloud some overall parameters can be given. These parameters can be used for analyzing the cloud and compare clouds in different situations.

2.5.1 Cloud Fraction

Both the stratocumulus and the cumulus are low clouds and have a typical height ranging from 500m till 2km. The difference between them is the density of the clouds. The stratocumulus is very dense and lumped together unlike the cumulus which is much more diffuse. Typical examples are shown in Figure 1 and Figure 2. The cloud fraction is the area fraction on a horizontal plane of grid cells that are cloudy. Stratocumulus has a typical cloud fraction of 100%. If the cloud fraction is much lower, there are cumulus clouds. These clouds have a typical cloud fraction of 10%.

A related variable is the cloud cover. The cloud cover is the part of the atmosphere that is covered by clouds. In models this is calculated by taking the fraction of columns in which there are one or more cloudy grid cells. The cloud cover for stratocumulus is typically 100% and in case of only cumulus typically 10%. This variable can therefore also be used to see if there is a breakup/transition.

2.5.2 Liquid Water Path

An second quantity for the clouds is the Liquid Water Path (LWP). It is defined as

$$LWP = \int_{z=0}^{z_{top}} \rho q_l dz. \quad (2.39)$$

Where ρ is the density and q_l is the liquid water content. If this value is high there will be more liquid water in the cloud column, leading to a more dense cloud. And as said earlier this is the case for stratocumulus clouds. A transition from stratocumulus to cumulus could be seen by a decrease of the LWP.

2.5.3 Buoyancy-flux Integral Ratio

The buoyancy-flux integral ratio (BIR) is introduced by Turton and Nicholls (1987). The BIR-value displays in indicates the degree of decoupling. The ratio is defined as

$$BIR \equiv - \frac{\int_{z < z_0 \text{ at which } \overline{w'\theta_v'} < 0} \overline{w'\theta_v'} dz}{\int_{\text{all other } z} \overline{w'\theta_v'} dz}. \quad (2.40)$$

where $\overline{w'\theta_v'}$ is the mean buoyancy flux. When BIR was introduced it was thought that it would give a threshold value, and if the value was higher, decoupling will occur. At the moment this value was introduced a threshold value of 0.4 was estimated. In 1997 Bretherton and Wyant showed that a threshold of 0.15 would be better. They used a Mixed Layer Model, this model shows that if the BIR exceeded 0.15, the BIR-value will keep

growing. The drawback of this test is that they use a Mixed Layer Model even when the assumptions of a well-mixed layer are not met. Later in 2000, Stevens showed that the boundary layer is unable to remain well mixed for $BIR > 0$, and for a $BIR > 0.1$ there will be a development of a two layer structure.

2.5.4 Moisture Flux Ratio

To get some more insight in the lifetime of the cloud a new variable, the ratio r_q , is introduced. This ratio is given by

$$r_q(z, t) = \frac{\overline{w'q_t'}_{at\ height\ z}}{\overline{w'q_t'}_{at\ surface}}. \quad (2.41)$$

This ratio can be used to get some quantitative idea of the amount of moisture that flows into the cloud.

The ratio r_q can also be used to linearize the moisture flux. The turbulent moisture flux can be linearized with respect to height in the Surface Mixed Layer (SML). This is the area from sea surface till the minimum cloud base, the lowest height where clouds are present. The used linearization is

$$\overline{w'q_t'}(z) = \overline{w'q_t'(ss)} \left(1 + \frac{(r_q(cb) - 1)z}{cb} \right). \quad (2.42)$$

Where cb is the cloud base height. This linearization can be very easily plugged in eq. (2.27). Removing the diffusion term, assuming horizontal homogeneity and taking the total derivative in this equation gives

$$\frac{d\overline{q_t}}{dt} = -\frac{\partial \overline{w'q_t'}}{\partial z} + S_{q_t}. \quad (2.43)$$

Substituting (2.42) in (2.43) gives

$$\frac{d\overline{q_t}}{dt} = \overline{w'q_t'(ss)} \left(\frac{1 - r_q(cb)}{cb} \right) + S_{q_t}. \quad (2.44)$$

The physical interpretation of the equation is if r_q is below 1 at minimum cloud base, the amount of moisture in the SML will increase. The mean cloud base height can be used to see the amount of moisture that reaches the cloud. The lifetime and albedo of the cloud is very dependent on the amount of water that reaches the cloud.

2.5.5 Buoyancy Flux Ratio

A similar analysis as the moisture flux ratio can be made for the buoyancy flux ratio. The turbulent virtual temperature flux ratio is given by

$$r_{\theta_v}(z, t) = \frac{\overline{w'\theta_v'}_{at\ height\ z}}{\overline{w'\theta_v'}_{at\ surface}}. \quad (2.45)$$

Like the moisture flux it is linear below the minimum cloud base in a single column. Due to averaging over the full grid some of the linear behaviour is smeared out in height and this will lead to a curved profile instead of a sharp peak as can be seen in Figure 6. This curved profile can be recalculated to a linear profile by linear extrapolation of the bottom 3/4 of the heat flux. The extrapolation is valid from the sea surface till the minimum cloud base. The rest of the analysis is similar to the moisture flux ratio. The tendency in the SML is

$$\frac{d\overline{\theta_v}}{dt} = \overline{w'\theta_v'(ss)} \left(\frac{1 - r_{\theta_v}(cb)}{cb} \right) + S_{\theta_v}. \quad (2.46)$$

The buoyancy flux ratio can be used to quantify the decoupling. In a well mixed the ratio will not become below 0. The lower the ratio the more decoupling there is.

2.6 Large Eddy Simulating

There are some different types and ways to calculate clouds and their behavior. The frequently used MLM is based on the assumption of a vertically mixed layer. It is also possible to model the cloud solving directly the Navier-Stokes equations. This can be done by Direct Numerical Simulation (DNS). DNS has a typical resolution of mm . For clouds this is computationally too intensive and therefore LES is used. By using LES the processes on the smallest scales that can not be solved are parameterized. On the larger scales LES solves the filtered conservation equations, because this is computationally less demanding.

The different models have different parameterizations. For example the parameterization for the precipitation, radiation and subgrid-scale turbulence could be different. The models are run on a total grid size of $4.48^2 km^2$ and a grid cell size of $5m \times 5m \times 35m$. DALES is also run with a different scale in the ASTEX case

with the total grid size $25.6^2 km^2$ and a grid cell size of $15m \times 15m \times 50m$. In the composite cases only DALES is used.

Table 2 List of the models participating and the modelers

Modeller	Model	References
A. Ackerman	DHARMA	Stevens <i>et al.</i> (2002)
P. Blossey	SAM 6.8.2	Khairoutdinov and Randall (2003)
A. Lock	MOLEM	Shutts and Gray (1994) Abel and Shipway (2007)
I. Sandu	UCLA LES	Stevens and Seifert (2008)
J. van der Dussen & S. de Roode	DALES	Heus <i>et al.</i> (2010)

3 Model results of cloud Transitions

3.1 Transition

3.1.1 Cloud Fraction

The cloud fraction can be used to see the characteristics of the transition. For the ASTEX case the cloud fraction and the cloud contours are given in Figure 7. The red squares display the observations from ASTEX. The

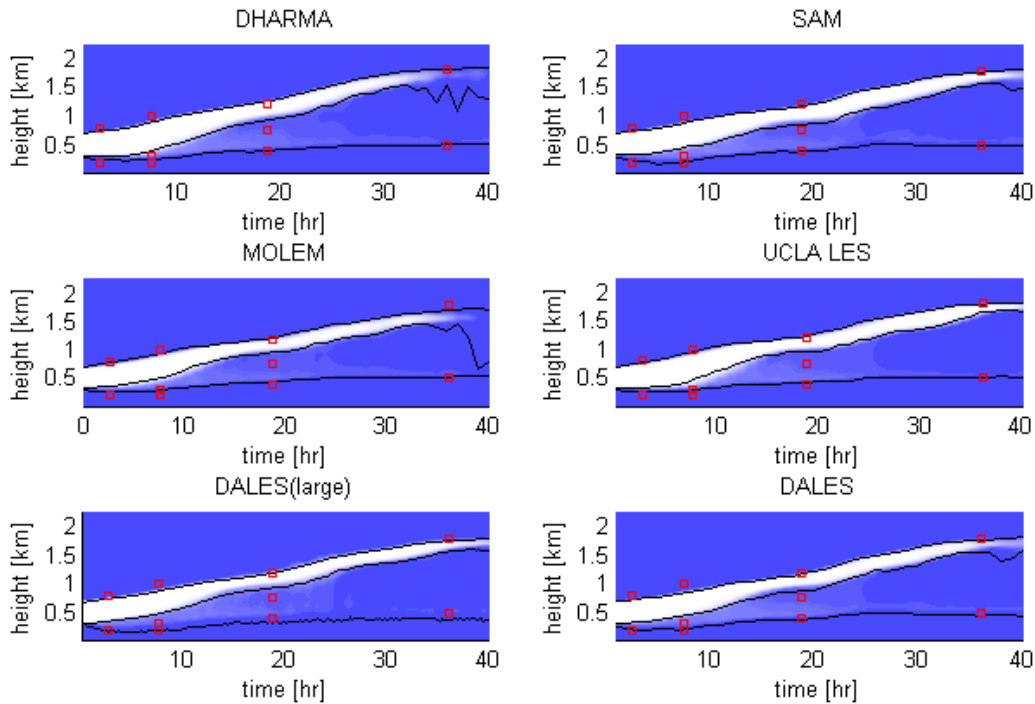


Figure 7 Cloud fraction and cloud contours in the ASTEX-case for different LES-models, the red squares are the observations from ASTEX. The used color map is in Figure 8.

transition can be seen in the decrease of the cloud fraction. Like the observations all stratocumulus clouds rise in time. Starting at an height of 700m the cloud top rise to approximately 1500m. Also the transition from stratocumulus to cumulus is rather good captured by the models. Around the 18th hour the cloud has a temporary minimum in cloud thickness. There are small differences between the models in the sub-cloud layer halfway the transition. At the end of the simulation the models differ in height and intensity of the clouds.

The composite cases are displayed in Figure 8. The composite cases also show an increase in cloud height.

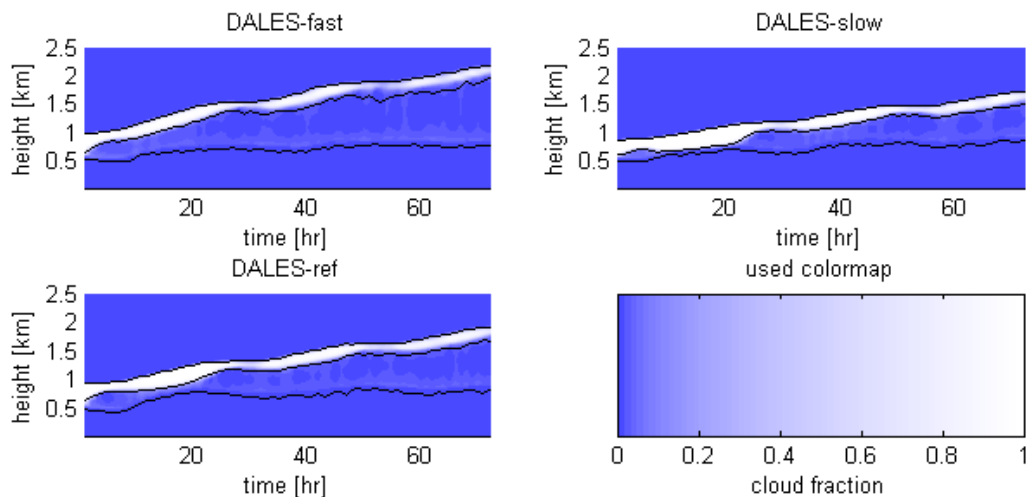


Figure 8 Cloud fraction in composite case

Another interesting observation is the small cloud fraction around the 30th. Around the 55th hour there is a similar pattern.

The cloud cover of all the cases is displayed in Figure 9. Especially in the ASTEX-case there is a cloud breakup, only the moment of breakup is different. The composite cases show a clear diurnal pattern by the lower cloud cover during the day, which indicates influence of radiation. The diurnal pattern can be best seen in the fast-transition case. After the second diurnal decrease in cloud cover, full cover is not reached, indicating the start of the breakup. The fast-transition case has the overall lowest cloud cover. Which is in agreement with the expectations, because this indicates a more progressed break up.

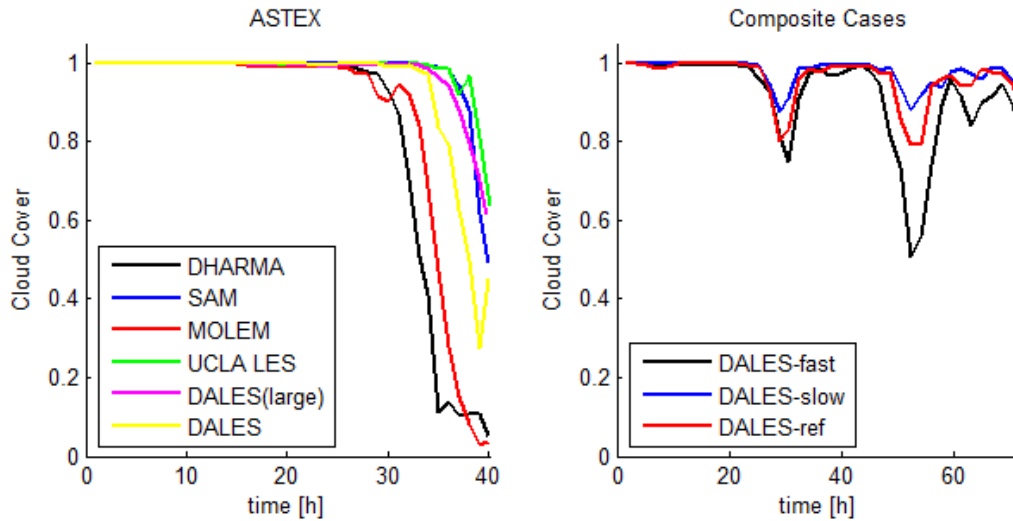


Figure 9 Cloud cover for all cases

As stated in the theory in 2.5.2, a transition of stratocumulus to cumulus is associated with a decrease in the LWP. The LWP for both the ASTEX and the composite cases are displayed in Figure 10. All the models show a decrease in LWP, therefore the transition is also confirmed by the LWP. The LWP is lower when the cloud is

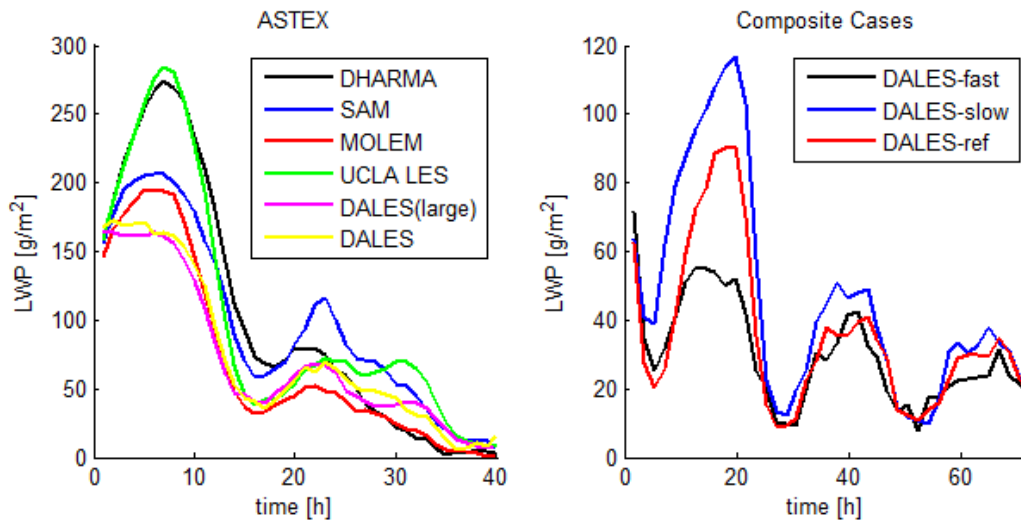


Figure 10 Liquid Water Path for all cases

thinner, the same holds for the cloud cover in the composite case. The correlation between LWP and cloud cover is not directly observed in the ASTEX-case. Probably because LWP-values below $40\text{g}/\text{m}^2$ indicate a breakup.

3.2 Decoupling

3.2.1 Result of Profiles

As stated in 2.4 the decoupling can be observed in the profile of the different fluxes. The profiles at the 18th hour are displayed in Figure 12. This is in harmony with the profiles in 2.4. For the moisture flux this relation is not so obvious. The moisture flux has no clear minimum at the negative buoyancy flux. To make it a

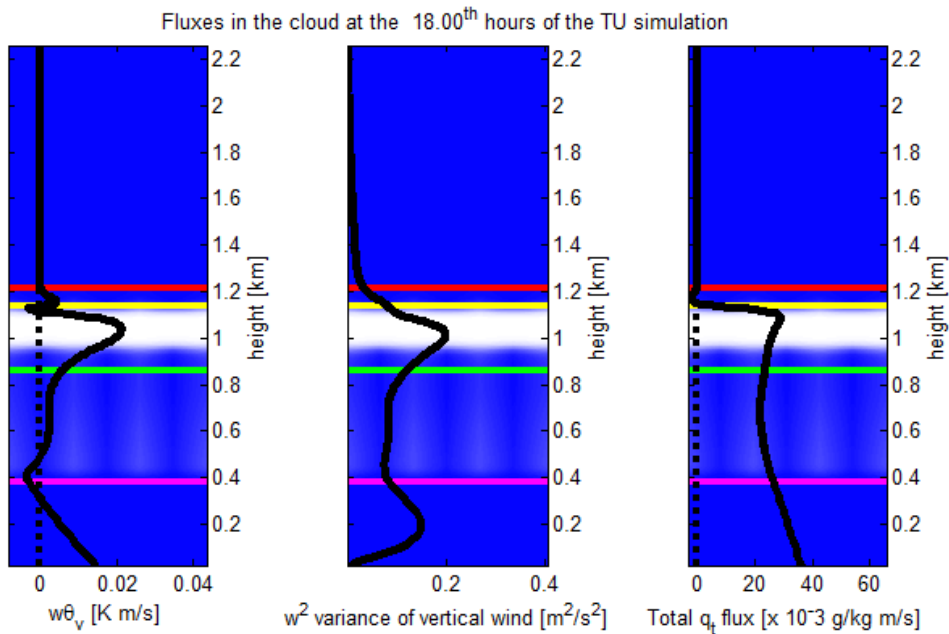


Figure 11 Relative low moisture flux during decoupling. Hourly main values of DALES. The horizontal lines indicate the cloud contours.

bit more clear a profile plot at another moment is displayed in Figure 11. The buoyancy flux is still negative at the minimum cloud base. Also the variance of the vertical wind is low, but the moisture flux is much higher compared with the sea surface. There is no a clear minimum at the minimum cloud base and also an increasing flux with height.

The conserved variables are q_t and θ_l . As explained in 2.4 would a non-flat profile indicate decoupling. The height of the decoupling is starting at 400m and increases till a height of 500m. This height is equal to the minimum cloud base height displayed in Figure 7.

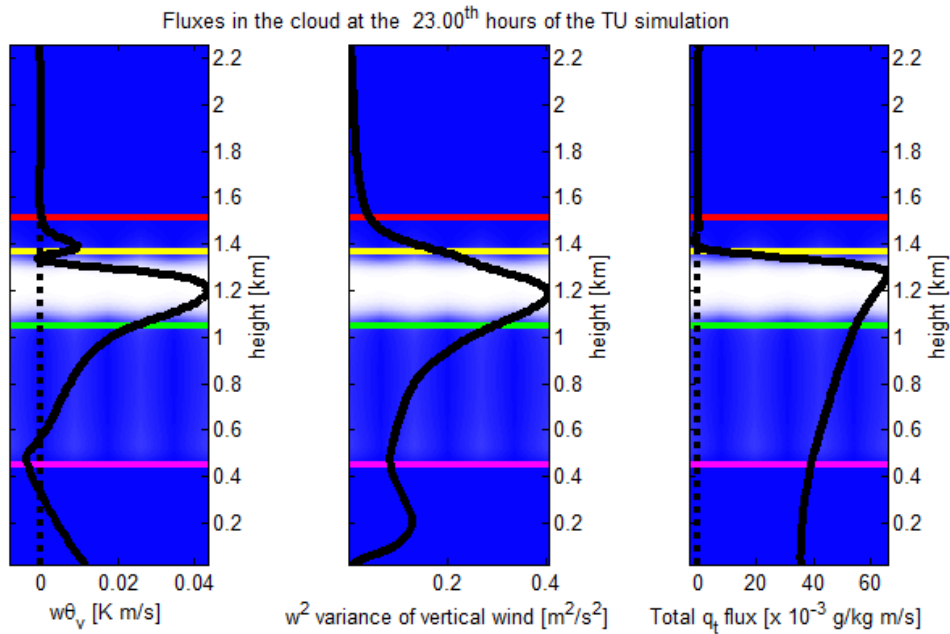


Figure 12 Relative high moisture flux during decoupling. Hourly main values of DALES. The horizontal lines indicate the cloud contours.

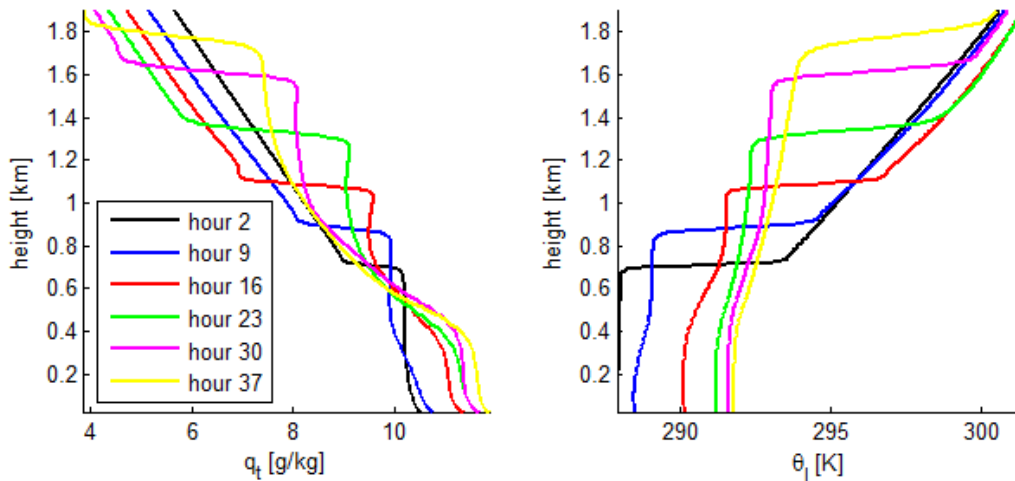


Figure 13 Profiles of the conserved variables in DALES for different times

3.2.2 Buoyancy Integral Ratio

The BIR-value can be found in Figure 14. Most of the models in the ASTEX-case show a fluctuating decreasing value. Except for the first 5 a 6 hours when an increasing value is observed. This can be explained by the initialization of the model. The first hours of the model are needed to initialize the model. In the composite cases there are some differences between the models. The slow-case is from the 10th hour till the 20th hour totally coupled according the BIR-value. After this period there is a negatively buoyant area. This negatively buoyant area is also observed in the reference-case. This very strong inversion layer would suggest a decoupled profile. Therefore this period will get some more consideration in the turbulent moisture flux ratio analysis.

After 25 hours in the composite cases, and after 10 hours in the ASTEX-case the BIR-value stays more or less constant or decreases in the transition, while there is decoupling observed. This provides support for the idea that the BIR-value can only be used as a threshold after which MLM is not valid. But in case there is decoupling more complex models have to be used to get a confident forecast.

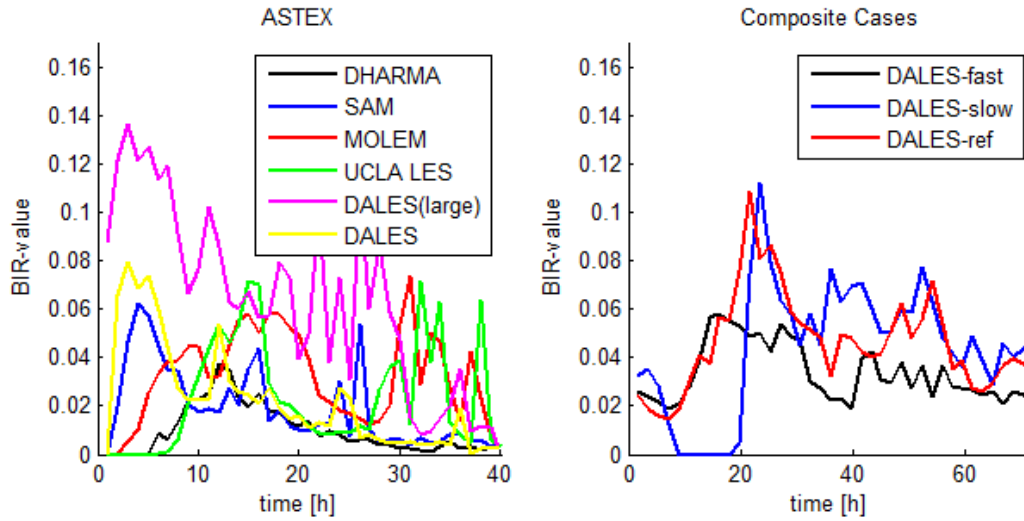


Figure 14 BIR-value for all cases

3.2.3 Buoyancy Flux Ratio

The results for the buoyancy flux ratio are shown in Figure 15. In the first hour there are very high ratios in the ASTEX-case. The explanation for these high values has to do with the initialization of the model. The buoyancy flux in the first hour is mainly dominated by the initial conditions of the model. In the slow transition case there is a similarity between the BIR-value and the buoyancy flux ratio. The ratio is high and the BIR-value is 0, both indicating a fully coupled layer. The ratio of MOLEM is not displayed in the graph. The buoyancy flux at the sea surface is very high and can be regarded as a outlier.

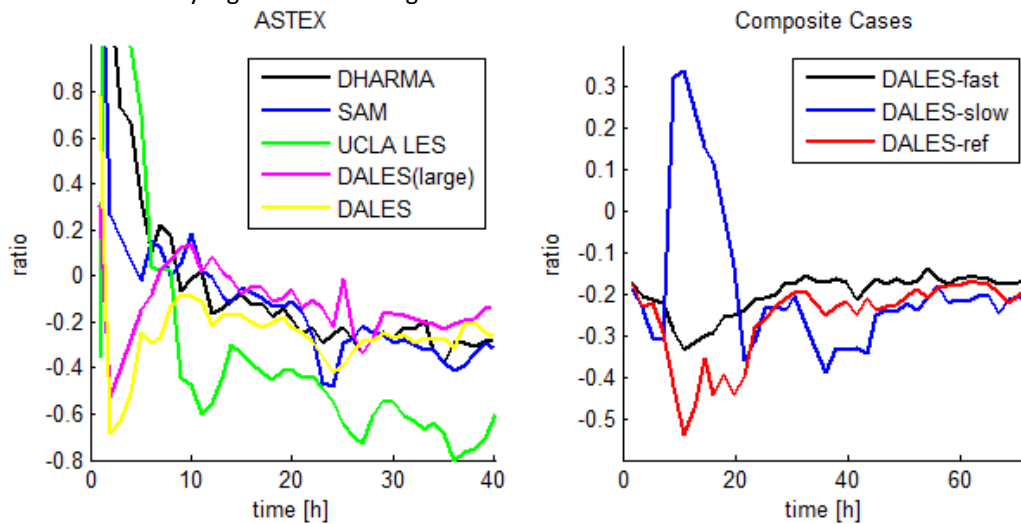


Figure 15 Buoyancy Flux Ratio for all models except the MOLEM-simulation

4 Turbulent Moisture Flux Ratio

4.1 Height dependence of the Turbulent Moisture Flux Ratio

The most important part of the analysis is the moisture flux. Therefore the moisture flux ratio defined in 2.5.4 is used. To apply the ratio in the analysis, the relevant height has to be chosen. There are different options for the height at which this ratio is defined. To take into account the decoupling the height have to be between the minimum cloud base and the mean cloud base. Between these two heights different criteria could be chosen. Some interesting options are: minimum cloud base, mean cloud base, minimum vertical turbulence, minimum buoyancy flux, minimum moisture flux, maximum moisture flux and halfway the mean and minimum cloud base height. The minimum and maximum moisture flux criteria display, by definition, the lower and upper bound of the ratio. In Figure 16 different criteria are plotted for the DALES-simulation. The difference between the lowest and highest ratio is most of the time below 0.4. An interesting result is that the ratio halfway the different cloud bases almost coincides with the minimum ratio. This points out that the minimum moisture flux is in the middle of the mean and minimum cloud base. A second remark can be made about the mean cloud base. The mean cloud base coincides most of the time with the maximum ratio. As shown in Figure 13 the SML is mixed from the sea surface till minimum cloud base height, also the moisture flux is linear in that area. These two conditions are needed to use the tendency equation for the humidity in (2.44). Therefore the minimum cloud base is chosen. The mean cloud base is chosen to see how much of the evaporated moisture at the sea surface reach the cloud.

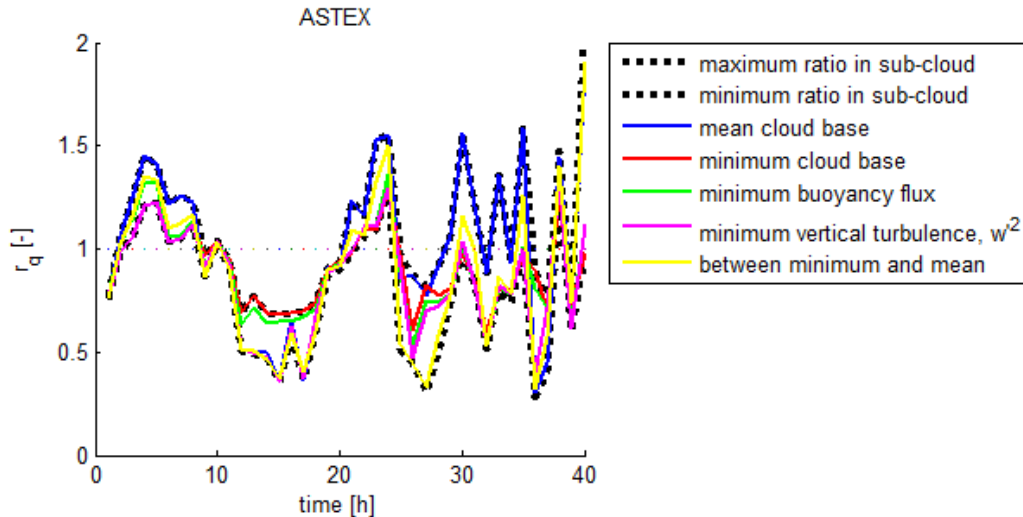


Figure 16 Ratio for different criteria

4.2 ASTEX results

The evolution of the surface fluxes is plotted in Figure 17. Both the moisture and heat flux change in time. The moisture flux is much higher from the 10th hour till the 25th hour. The explanation for this result is the increase in horizontal wind velocity. The heat flux at sea surface has a peak at the 10th hour.

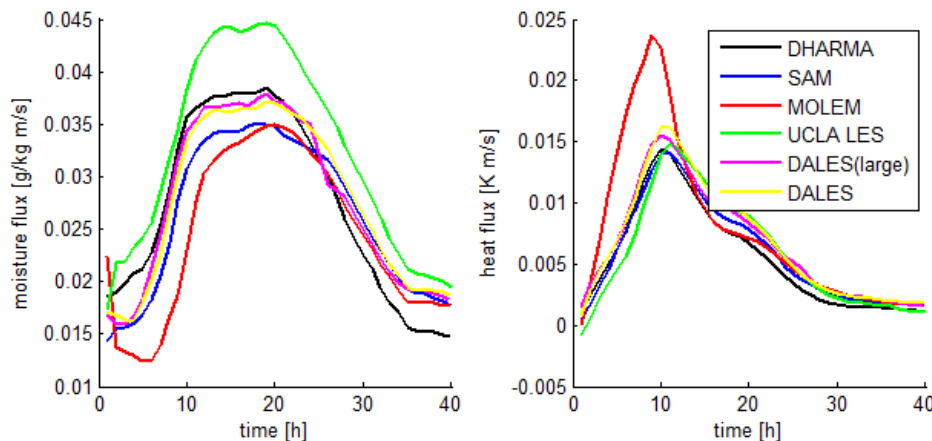


Figure 17 Evolution of surface fluxes in ASTEX

The moisture ratio for the ASTEX-case is displayed in Figure 18. The first important observation is the similar behavior for the ratio in the different models. During the first 20 hours the models give similar ratios. In the last 15 hours the models are significantly different. The overall form is in all models the same, that is to say the ratio has a period oscillation. The frequency of this oscillation is around 24 hours, which indicates a high dependency on the radiation of the sun. The last interesting observation is the mean ratio. The mean ratio at minimum cloud base taken over different models is 0.89. At the mean cloud base, which by definition is located higher, this ratio is 0.99. The lowest observed ratio is 0.07 in the UCLA LES model.

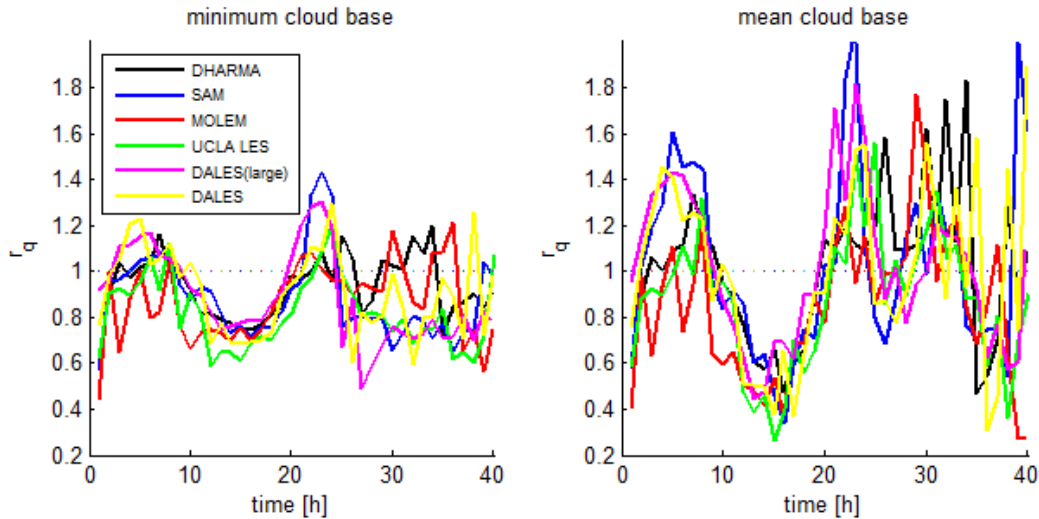


Figure 18 Moisture Ratio in ASTEX-case

At the start of the simulation all the models contain the same amount of water as restricted by the initial condition. At the start of the simulation the specific humidity at the SML and the cloud are almost equal, indicating a good mixing from the sea surface till the cloud top. In time the humidity of the cloud and the SML starts to differ. Both Ackerman and Lock show an increasing humidity after a period of decreasing humidity in the cloud. This is likely to be linked to the breakup which is earlier in these models as can be seen in Figure 9. An extra effect, not shown here is the precipitation leading to a decrease in the total water content in the CTBL. In the first 10 hours there is a significant effect of the precipitation, after 10 hours precipitation is negligible. In time the surface mixed layer (SML) becomes a bit wetter. This could partly be explained by the increasing sea surface temperature. An increasing temperature leads to a higher saturation value and thereby an increasing

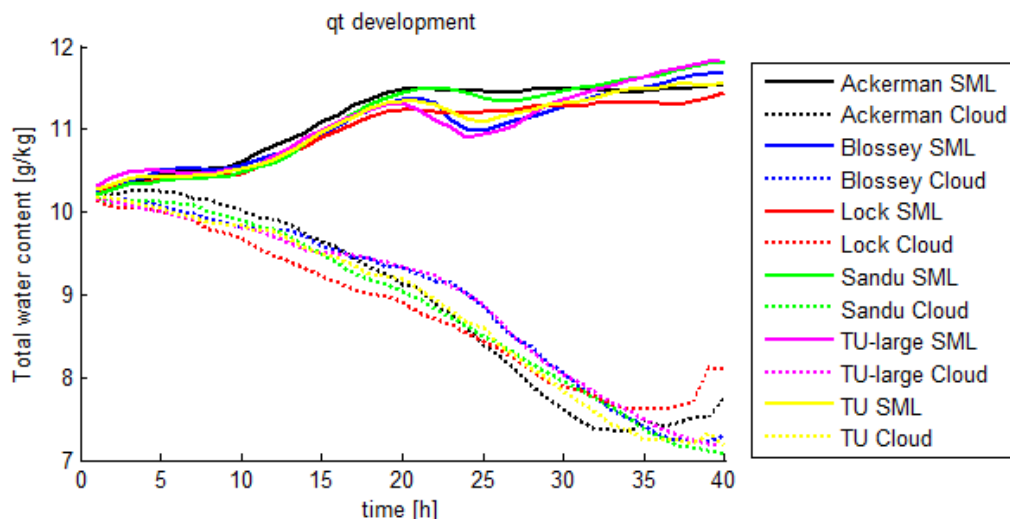


Figure 19 Evolution of water content

humidity. The other important effect is the increase in evaporation at the sea surface as can be seen in Figure 17. The moisture flux from the sea surface partly reach the cloud above the SML, summarized in the moisture flux ratio in Figure 18. Due to decoupling the SML will wet and the ascending stratocumulus cloud dry.

4.3 Composite Cases results

The evolution of the surface fluxes is plotted in Figure 20. Both the moisture and heat flux change in time. The moisture flux shows an increasing behavior. Besides this increasing flux there is a day-night pattern. During the day, the surface fluxes are typically lower than during the night.

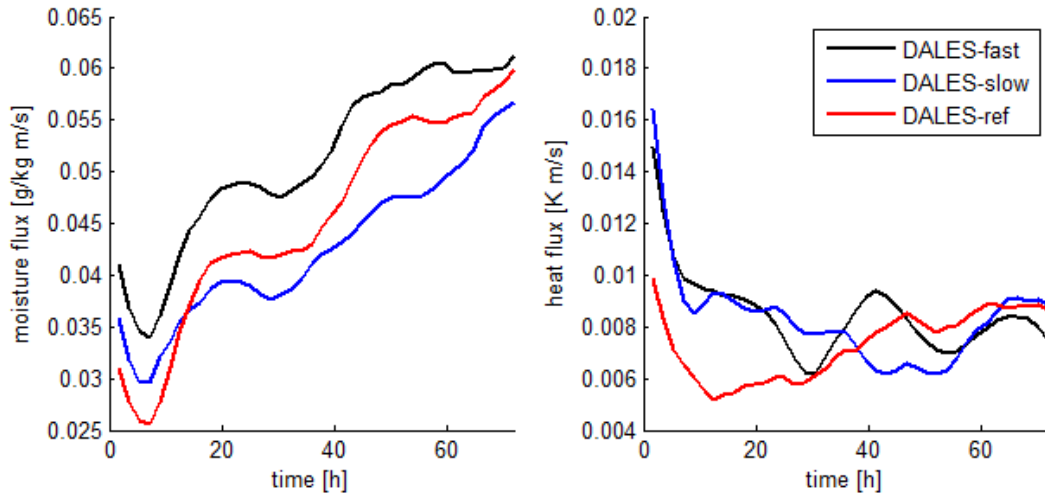


Figure 20 Evolution of surface fluxes in composite cases

The ratios for the composite cases are displayed in Figure 21. Same as for the ASTEX-case there is a clearly observable day-night pattern. So the ratio in all the cases is significantly dependent of the sun. As could be seen in Figure 14 there was a relatively high value for the BIR around 25 hours. Especially the reference and slow case show this high BIR-value. This coincides with a low ratio at the minimum cloud base. Also at the mean cloud base there is a minimum. The mean ratio at minimum cloud base taken over different cases is 0.85. At the mean cloud base the ratio is 0.78. The observed ratio drops never below 0.28 in the three cases.

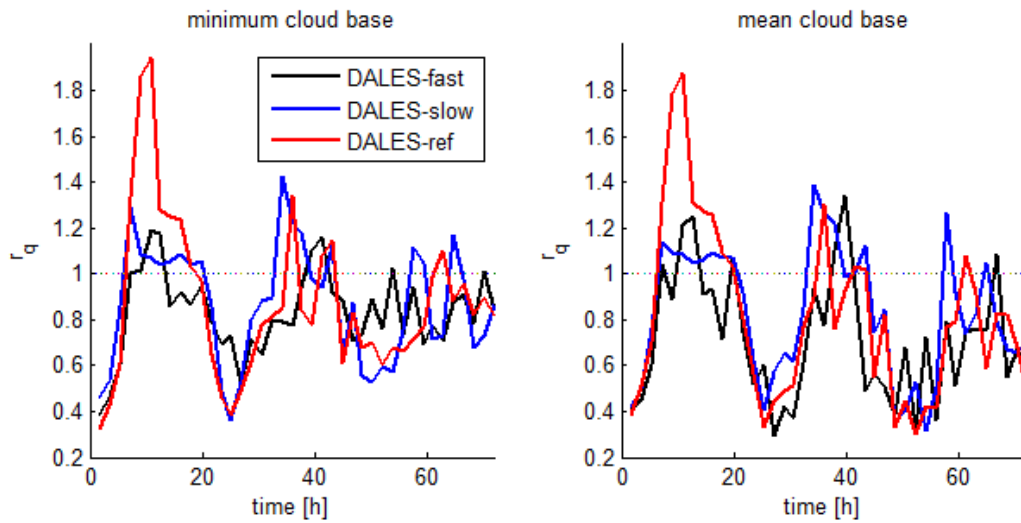


Figure 21 Moisture Ratio in composite cases

The development of the amount of moisture is displayed in Figure 22. At the start of the simulation the humidity at SML and cloud are almost equal in the different cases. Equal humidity indicates a good mixing from the sea surface till the cloud top. The cloud dries a bit and has a diurnal pattern. This pattern is anti-correlated with the humidity in the SML. In time the surface mixed layer becomes a bit wetter. This could at least partly explained by the increasing sea surface temperature. An increasing temperature leads to a higher saturation value, thereby the surface flux will increase as shown in Figure 20. This is equal to the situation in the ASTEX-case. Because the composite cases are run for 3 days, it is also possible to extract some linear effects, for example the increasing sea surface temperature. The result is shown in Figure 23 . The similarity with Figure 21 is easily seen. The conclusion made on basis of these two figures is a buildup of moisture during the day in the SML. During night this is released to the layers above.

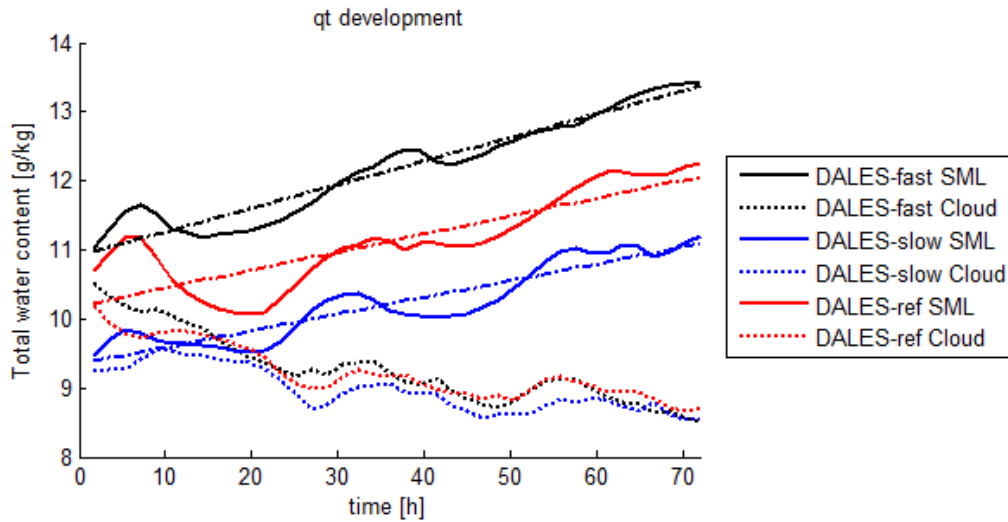


Figure 22 Humidity development in the composite cases

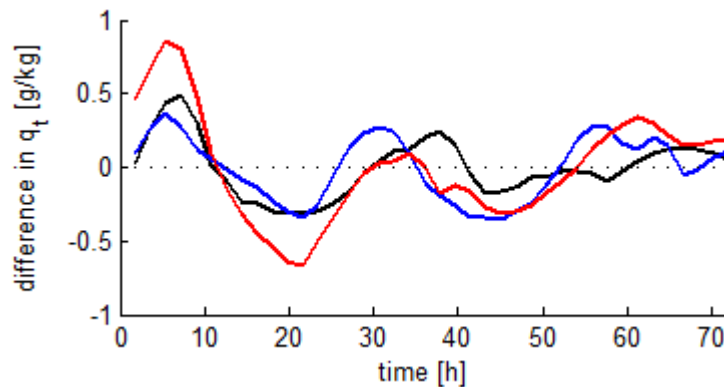


Figure 23 Difference between q_t in the SML and a linear trend, the used colors for the different cases are the same as in Figure 22

5 Conclusions and Recommendations

5.1 Conclusions

The simulations capture the transition of stratocumulus to cumulus. The decoupling is observed through the structure in the profiles of the conserved variables, q_t and Θ , the variance of vertical wind and the buoyancy flux. The moisture flux profile does not show a clearly decoupled profile.

The BIR-value gives a rather good indication for the decoupling of the buoyancy and the variance profiles. For the moisture flux the relation with the BIR-value is not so clear.

The moisture flux has a day-night pattern. This indicates a high dependence of the sun radiation. The resulting moisture ratios are in the ASTEX-case: 0.89 at minimum cloud base and 0.99 at mean cloud base. The lowest ratio is 0.07. In the composite cases is the minimum cloud base 0.85 and the mean cloud base 0.78. The lowest ratio is 0.28. The ratio is always higher than zero in all the cases. There is a buildup of moisture in the SML during day and during the night this is released to the layers above. A summarizing view is in Figure 24.

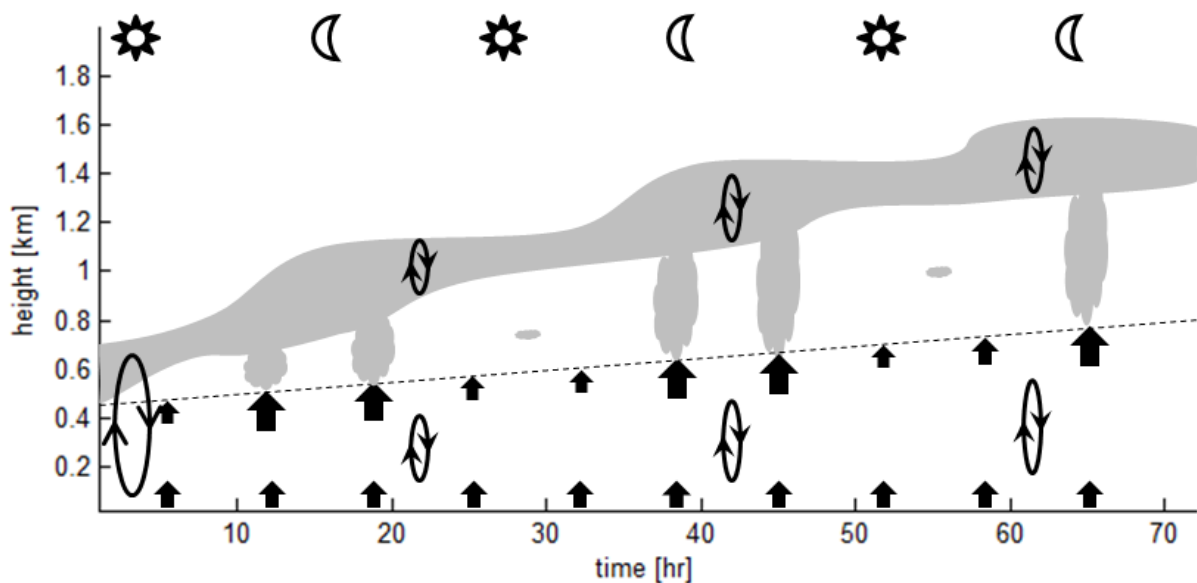


Figure 24 An overview of the obtained results. The line width of the arrows indicate the amount of moisture transport. The circled lines indicate the mixing.

5.2 Recommendations

To get decoupling there has to be a negative buoyancy flux. As can be seen in eq. (2.34) and in eq. (2.35) the buoyancy flux is dependent on the moisture flux, the heat flux and on the presence of liquid water. As the moisture flux will be positive most of the time, the heat flux has to be negative to get a negative buoyancy flux. Therefore the whole system is very sensitive to fluctuations in the heat flux. It would be interesting to run the case using different parameterizations for the heat flux at the sea surface because this boundary condition can influence the whole system.

Because it takes some time for 'information' to travel through the cloud it would be interesting to see if there is a time lag. For example between the ratio in the minimum cloud base and the mean cloud base. A more negative buoyancy flux at the minimum cloud base could have a decreasing effect on the ratio at the mean cloud base a bit later. In Stull (1993) it is suggested that a thermal needs 5 to 15 minutes to cycle between the bottom and the top. It would be interesting to see whether LES-models support this idea.

To get a better insight in the results, a correlation between humidity in the SML and could be obtained. In both the humidity and the ratio is a diurnal pattern. Maybe also a time lag can be found.

The amount of turbulent moisture transport from minimum cloud base to mean cloud base is time dependent. The cloud fraction in this layer does not correlate with the turbulent moisture transport at first sight. The difference in turbulent moisture transport is due to wetter clouds, more turbulent clouds or lies outside the cloud. Sampling on cloudy grid cells and comparing with non-cloudy grid cells can be interesting.

6 Bibliography

- P. Bougeault. The Diurnal Cycle of the Marine Stratocumulus Layer: A Higher-Order Model Study. *Journal of Atmospheric Sciences*, 42: 2826-2843, 1985.
- C.S. Bretherton and M.C. Wyant. Moisture Transport, Lower-Tropospheric Stability, and Decoupling of Cloud-Topped Boundary Layers. *Journal of the Atmospheric Sciences*, 54: 148-167, 1997
- T. Heus, CC van Heerwaarden, H.J.J. Jonker, A.P. Siebesma, S. Axelsen, K van den Dries, O Geoffroy, A.F. Moene, D. Pino, S.R. de Roode, J. Vil-Guerau de Arellano. Formulation of the dutch atmospheric large-eddy simulation (dales) and overview of its applications. *Geosci. Model Dev.* 3:415-444, 2010
- M.F. Khairoutdinov, D.A. Randall. Cloud resolving modeling of the arctic summer iop: Model formulation, results uncertainties, and sensitivities. *Journal of the Atmospheric Sciences*, 60: 607-625, 2003.
- G.M. Martin, D.W. Johnson, D.P. Rogers, P.R. Jonas, P. Minnis, D.A. Hegg. Observations of the interaction between cumulus clouds and warm stratocumulus clouds in the marine boundary layer during ASTEX. *Journal of the Atmospheric Sciences*, 52: 2902-2920, 1994.
- S. Nicholls. The dynamics of stratocumulus: aircraft observations and comparisons with a mixed layer model. *The Quarterly Journal of the Royal Meteorological Society*, 110: 783-820, 1984.
- S.R. de Roode. *Cloudy boundary layers. Observations and mass-flux parameterizations*. PhD thesis, University of Utrecht, 1999.
- S.R. de Roode. *Clouds*. University of Utrecht, 2004.
- I. Sandu, B. Stevens. Description of the Lagrangian composite cases.
- I. Sandu, B. Stevens, R. Pincus. On the transitions in marine boundary layer cloudiness. *Atmos. Chem. Phys.*, 10: 2377-2391, 2010.
- G.J. Shutts, M.E.B. Gray. A numerical modeling study of the geostrophic adjustment process following deep convection. *The Quarterly Journal of the Royal Meteorological Society*, 120: 1145-1178, 1994.
- B. Stevens. Cloud transitions and decoupling in shear-free stratocumulus-topped boundary layers. *Geophysical Research Letter*, 27: 2557-2560, 2000.
- B. Stevens, A.S. Ackerman, C.S. Bretherton. Effects of domain size and numerical resolution on the simulation of shallow cumulus convection. *Journal of the Atmospheric Sciences*, 59: 3285-3301, 2002.
- B. Stevens, A. Seifert. Understanding macrophysical outcomes of microphysical choices in simulations of shallow cumulus convection. *J. Meteor. Soc. Japan* 86A: 143-162, 2008.
- R.B. Stull. *An Introduction to Boundary Layer Meteorology*. Kluwer Academic Publishers, 1993.
- J.D. Turton and S. Nicholls. A study of the diurnal variation of stratocumulus using a multiple mixed layer model. *The Quarterly Journal of the Royal Meteorological Society*, 113: 969-1009, 1987.
- Wood, Robert, Christopher S. Bretherton. Boundary Layer Depth, Entrainment, and Decoupling in the Cloud-Capped Subtropical and Tropical Marine Boundary Layer. *Journal of Climate*, 17: 3576-3588, 2004.

7 Appendix A

Reynolds Decomposition and Averaging

Reynolds decomposition is splitting a variable, φ in a mean, $\bar{\varphi}$, and a turbulent part, φ' . Adding both parts gives the original variable, $\varphi = \bar{\varphi} + \varphi'$. The idea behind this decomposition is to split the turbulent flow from the total flow.

Reynolds averaging is taking the average of the variable. By taking the average over a decomposed variable only the mean part remains. The average of the turbulent part is zero, $\overline{\varphi'} = 0$. Using these assumptions, the following equations can be obtained

$$\overline{a + b} = \bar{a} + \bar{b} \quad (4.1)$$

$$\bar{a} = \overline{(\bar{a} + a')} = \bar{a} + \overline{a'} \quad (4.2)$$

$$\overline{a \cdot b} = \overline{(\bar{a} + a') \cdot (\bar{b} + b')} = \bar{a} \cdot \bar{b} + \overline{a' \cdot b'} \quad (4.3)$$

These tools are based on a separation of length scale. 'In practice, this means that if one makes a Fourier transformation of a quantity, its spectrum is assumed to have a distinct minimum intensity at scales between ~ 1 and ~ 10 km,'(Roode, 2004). For the vertical velocity fluctuations this spectrum gap can be observed, but for other quantities this gap is not observed.

